Instructions to Authors for the Preparation of Papers for the 18th Australian International Aerospace Congress

Please select category below:

Normal Paper ☐

Student Paper ☒

Young Engineer Paper ☐

Detection and location of defects in rolling element bearing using acoustic emission

F. Larizza [1*], C.Q. Howard [1], S. Grainger [1] and W. Wang [2]

[1] *University of Adelaide, Adelaide, Australia*
[2] *DST Group, Melbourne, Australia*
** francesco.larizza@adelaide.edu.au*

Abstract

Rolling element bearings become worn and eventually fail by developing surface defects, such as spalls, dents and pits. Researchers have developed many methods to detect and estimate the size of defects in rolling element bearings. However, these methods do have limitations, such as when a defect with a circumferential length that is larger than the separation angle of the rolling elements cannot be distinguished from a smaller defect, and they cannot be located on the contact surfaces. This work presents a method to detect and locate defects in an operational bearing as it degrades over time, using the time delay between signals from several acoustic emission sensors. Experiments involved putting abrasive garnet into the bearing grease to accelerate the failure of the bearing, which could occur in practice from a defective seal.

Keywords: Rolling element bearing, Vibration condition monitoring, Acoustic emission

Introduction

The most common way bearings fail is by the formation of surface defects from the growth of fatigue cracks or the removal of surface grains during operation. Bearing defects can occur due to insufficient lubrication and high contact stresses between the rolling element and the raceways of the bearing, causing spalls, dents and pits to form on the contact surfaces [1]. These defects cause the contact force between the rolling element and the raceways to differ, causing the relative distance from the inner ring to the outer ring to vary from normal, resulting in higher than normal vibration amplitudes. Typical vibration condition monitoring involves trending the increase in vibration amplitude of a defective bearing. It is assumed that an increasing trend in vibration amplitude means that the defect size is increasing, but does not provide information about the actual size of the defect. However, to better manage the risk of a bearing that is failing, some industries have implemented regulations that specify the maximum allowable defect size in a bearing. Hence, it is desirable to determine the actual size of a defect in an operational bearing from its vibration response [2].

Many methods that estimate the size of a defect in an operational bearing have been

developed using the vibration response or the Acoustic Emission (AE) from a defective bearing [3-10]. Some methods use the time between key vibration characteristics as a roller passes through the defect zone to determine the size of the defect [3-5], whereas methods that use AE use the burst duration and the amplitude of the strain wave to estimate the defect size [6-10]. The ring-down count and the amplitude of the AE can be used to detect even the smallest defects like cracks in an operational bearing. These methods have a limitation in that they cannot distinguish between a defect that is greater than the separation angle of the rolling elements and one that is smaller than it, and the methods cannot locate the defect on the stationary ring. The defects used in the work presented in references [3-10] were artificially created by machining the raceway, or from a machined defect that was grown in size by operational use.

The work presented here involved creating a defect by contaminating the bearing grease, which could occur in practice from a defective seal, and then operating the bearing under load, causing the rolling elements to embed the contaminants into the raceways and form dents. Shear waves are generated as damage occurs to the bearing and as the rollers pass through the defect zone this is recorded by AE sensors. The time delay between the signals from AE sensors are used to determine the location of the damage on the raceway, and the amplitudes of the signals are indicative of the severity of the damage.

Previous Work

The size of a defect in an operational bearing can be determined by measuring the vibration response of the housing and using the time between key vibration features in the signal. However, these methods do have limitations such that, if the size of the spall defect is greater than the separation angle of the rolling elements, it is not possible to distinguish between a line spall and an extended spall defect using just time-series data. It was hypothesised and analytically shown by Petersen et al. [11] that the change in the bearing assembly stiffness can be used to determine if a defect is greater than the separation angle, as the bearing stiffness for the bearing with the extended spall defect is lower than the bearing with a line spall defect. However, this method was not verified experimentally.

References [6-10] show that traditional condition monitoring methods can be used to detect and estimate the size of line spall defects. For example, AE signals are generated by failure mechanisms such as crack propagation, friction and plastic deformation, and not the vibration response of the housing, as the frequency response of the housing is less than 100 kHz and failure mechanisms is greater than 100 kHz. Therefore, structural health monitoring techniques can be used to detect, locate and estimate the size of a defect in an operational bearing. Work presented by Elforjani and Mba [12, 13], used AE to detect and locate a spall defect in a bearing. The bearing used was a modified thrust ball bearing, where a flat raceway replaced one of the grooved raceways from a cylindrical roller thrust bearing, and the bearing was run-to-failure. Since the contact pressure on the flat raceway is much higher than the grooved raceway, spall defects began to form on the flat raceway. As the bearing degraded over time, the origin of the shear-waves due to crack propagation and plastic deformation was calculated, and the result showed that the location and the size of a single spall defect, or even multiple spall defects, could be determined. However, the shaft speed during the experiments was only 72 rpm, which is very low compared to typical shaft speeds that are around 1500 rpm.

The work presented here aims to extend the work by Elforjani and Mba [12, 13], by using a statistical approach to determine the location and severity of dent defects in a rolling element bearing caused by contaminants in the lubrication, at high shaft speeds.

Experimental Method

To accelerate the failure of a bearing, abrasive garnet was mixed into the grease before the bearing was packed and assembled on to the shaft. Contaminants mixed with grease could occur in practice from the failure of the bearing seal. The loaded rollers cause the contaminants to be pushed into the raceways and form dents.

Figure 1 shows the experimental setup and the position of the four AE sensors (Physical Acoustics F15A sensors with 2/4/6C preamplifiers) on the bearing housing. The experimental test platform is a modified SpectraQuest Bearing Simulator. The load was applied using a hydraulic piston and measured with a load cell. The shaft in Figure 1 (b) was rotating clockwise, and a tachometer was used to measure the shaft speed. The four AE sensors were located on the housing of the bearing with one sensor positioned on each of the positive and negative y-axis, one on the positive x-axis, and a fourth sensor positioned 17° before the positive y-axis, as shown in Figure 1 (b). Table 1 lists the locations of the sensors, where zero is the positive x-axis, and the measurements are taken in an anti-clockwise direction. The signals from the sensors were recorded with a sampling frequency of 2.926 MHz on an oscilloscope (PicoScope 5000). The sensors were attached to the bearing housing using (super-glue) cyanoacrylate mixed with crushed garnet to create a paste. This paste electrically isolated the sensors from the housing and the electric motor, which prevented ground-loops from occurring.

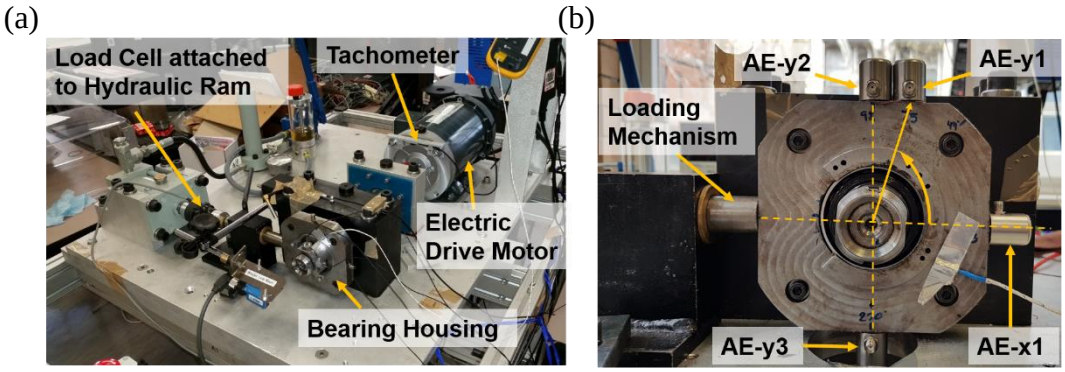

Figure 1: (a) Photo of the bearing test rig used to capture the dynamic response of a defective bearing. (b) Photo of the test bearing housing with all the measurement sensors.

Table 1: Sensor locations.

Sensor	Position (°)
AE-x1	-3
AE-y1	75
AE-y2	92
AE-y3	270

The bearing used in the experiment was a FAG N206E.TVP2 cylindrical roller bearing. Table 2 lists the specifications of the test bearing. The bearing was operated for a total of six hours, with an applied load of 10 kN, at a shaft speed of 20 Hz (1200 rpm). The signals from the sensors were sampled every fifteen minutes, for eight seconds. After every hour, a small amount of fresh garnet was added to the grease to simulate contaminates entering the bearing, and as the garnet became crushed into very fine powder over time, it was less effective in causing damage.

Table 2: Cylindrical roller bearing dimensions and specifications

Parameter	Value
Number of Rollers	13
Separation Angle (°)	27.7
Roller Diameter (mm)	9
Pitch Diameter (mm)	46.5
Dynamic Load Capacity (kN)	44

Results and Discussion

The response from the AE sensors was processed by taking the Kurtogram for each of the channels to determine the best frequencies to band-pass filter the signals, and the most appropriate window to scan the signal for impulses. Figure 2 shows the Kurtogram for the negative y-axis AE sensor (AE-y3) after 3 hours of operation, where the centre frequency of the band-pass filter was found to be 207.5 kHz, with a bandwidth of 1.5 kHz and a window size of 1024. After the Kurtograms are calculated, the signals from these channels are band-pass filtered and, in this case, a sliding window of 1024 samples is moved across the signal, looking for impulse peaks that are greater than three standard deviations above the mean of the signal.

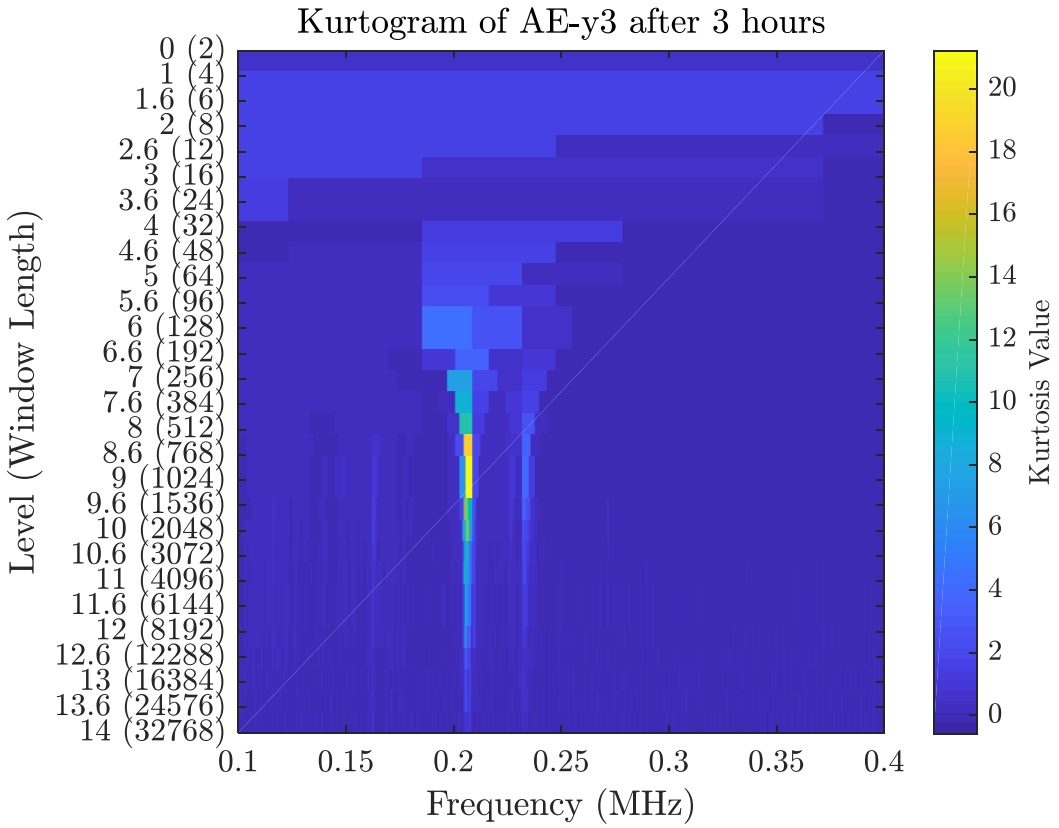

Figure 2: Kurtogram of the AE sensor AE-y3 after 3 hours of operation, where the maximum kurtosis value was found to be 21.3, with a centre frequency of 207.5 kHz, a bandwidth of 1.5 kHz and a window size of 1024.

When an impulse is identified, the time delay between the impulses measured by the sensors is determined, and the location of the origin of the wave is calculated. The origin of the wave is calculated by first determining the speed of the wave, which is calculated by using the time between the positive y-axis sensor response and the sensor that is 17° before it. After the speed of the wave is calculated, the time delay between the sensors on the positive and negative y-

axis is used to determine the origin of the impulse.

Figure 3 shows (a) a histogram of the calculated origins of the impulse measured by the AE sensors, and (b) panoramic photograph of the damaged raceways of the bearing after 6 hours of operation, formed by "stitching" multiple photos. The histogram shows that the majority of the impulses occurred at 180°, which is at the centre of the load zone and is to be expected, as this is where the greatest damage is likely to occur on the fixed outer raceway. This is evident as the larger dent defects are concentrated around the centre of the load on the outer raceway, as shown in Figure 3 (b). It can be seen that there is a second peak in the histogram at 0° and 360°, which is at the centre of the unloaded portion of the bearing. This result was unexpected as the rolling elements are unloaded in this region, and there should be little damage. When the outer raceway was inspected, there was wear in the unloaded portion of the bearing, as shown in Figure 3 (b). It was found from further investigation that as the garnet was premixed into the grease, the garnet removes the radial clearance of 25 – 45 micron in the bearing. This essentially preloads the bearing causing the damage on the unloaded section of the bearing as the rolling element embeds the garnet into the contact surface.

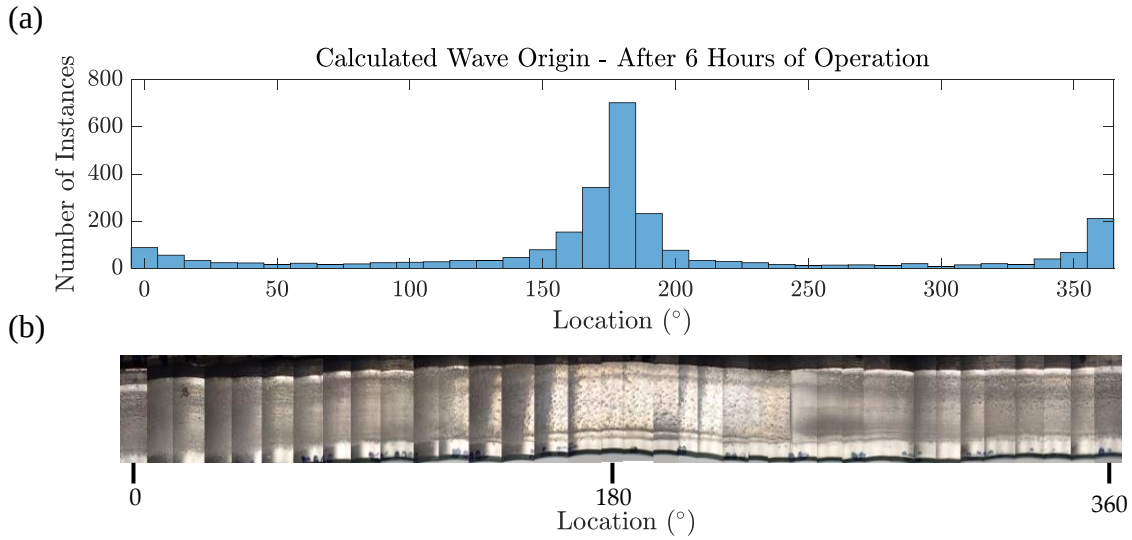

Figure 3: Histogram of the calculated wave origin during the test period and a photograph of the unwrapped outer raceway.

When the inner raceway and the rolling elements were inspected, it was found that there was minimal damage to both, as shown in Figure 4. The contact surface of the inner raceway and the rolling element have a matte surface finish with some pitting, but this damage is minor compared will the outer raceway and is representative of normal wear.

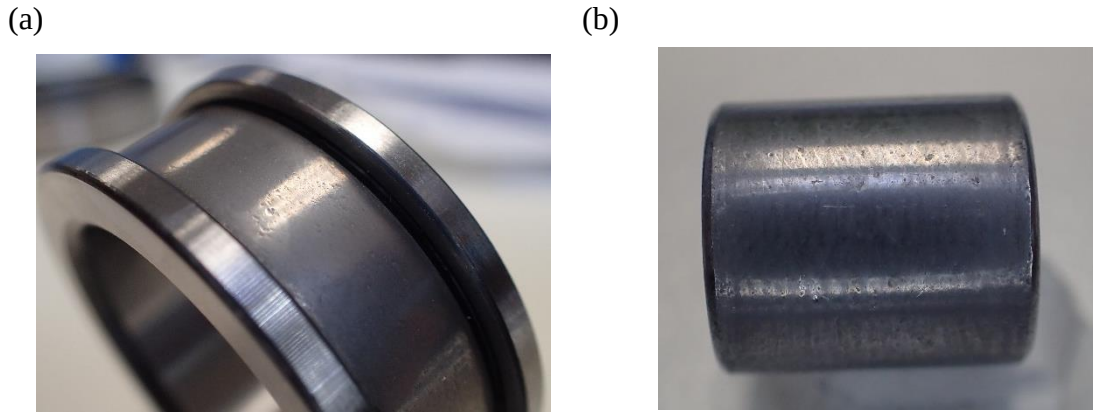

Figure 4: Photographs of the inner raceway and a rolling element after 6 hours of operation with contaminated grease.

Conclusion

This paper extends the work by Elforjani and Mba [12, 13], who conducted measurements of a defective bearing using AE sensors when the shaft on a bearing was rotating at 72 rpm. In the work presented here, a shaft was rotating at 1200 rpm that was supported by a cylindrical roller bearing under load. The bearing underwent accelerated fatigue testing, by adding abrasive garnet to the grease, which would simulate the process of a seal failure and contaminants entering the bearing. The location of the damage to the stationary outer raceway was determined by using AE sensors and signal processing. It was shown that the relative severity of damage to the raceway could be determined by using statistical analysis. Future work would be to include varying constant speed and load with contaminates present in the lubricate, and investigating if this method can be used to determine the location of spall defects on the inner and outer raceway of a bearing.

Acknowledgements

Acknowledgements to the Defence Science Institute for providing funding of this research, and the Australian Government for the Australian Post-Graduate Award.

References

1. Randall, R.B., *Vibration-Based Condition Monitoring*. 2011: John Wiley and Sons Ltd.
2. Tedric A. Harris, M.N.K., *Rolling Bearing Analysis, Fifth Edition - 2 Volume Set*. 2006: CRC Press.
3. Moazen-ahmadi, A. and C.Q. Howard, *A defect size estimation method based on operational speed and path of rolling elements in defective bearings.* Journal of Sound and Vibration, 2016. **385**: p. 138-148.
4. Sawalhi, N. and R.B. Randall, *Vibration response of spalled rolling element bearings: observations, simulations and signal processing techniques to track the spall size.* Mechanical Systems and Signal Processing, 2011. **25**: p. pp. 846-870.
5. Wang, W., N. Sawalhi, and A. Becker, *Size Estimation for NaNatural Occuring Bearing Faults Using Synchronous Averaging of Vibration Signals.* Journal of Vibration and Acoustics, 2016. **138**(5): p. 051015.
6. Mba, D., *The use of acoustic emission for estimation of bearing defect size.* Journal of Failure Analysis and Prevention, 2008. **8**: p. pp. 188-192.
7. Al-Dossary, S., R.I.R. Hamzah, and D. Mba, *Observations of changes in acoustic emission waveform for varying seeded defects sizes in rolling element bearing.* Applied Acoustics, 2009. **70**: p. pp. 58-81.
8. Al-Ghamdi, A.M., et al., *Estimation of bearing defect size with acoustic emission.* Journal of Failure Analysis and Prevention, 2004. **40**: p. pp. 188-192.
9. Kilundu, B., et al., *Cyclostationarity of acoustic emissions (AE) for monitoring bearing defects.* Mechanical Systems and Signal Processing, 2011. **25**: p. pp. 2061-2072.
10. Eftekharnejad, B., et al., *The application of spectral kurtosis on acoustic emission and vibrations from a defective bearing.* Mechanical Systems and Signal Processing, 2011. **25**: p. pp. 266-284.
11. Petersen, D., C. Howard, and Z. Prime, *Varying stiffness and load distributions in defective ball bearings: analytical formulation and application to defect size estimation.* Journal of Sound and Vibration, 2015. **337**(0): p. 284-300.
12. Elforjani, M. and D. Mba, *Natural mechanical degradation measurements in slow speed bearings.* Engineering Failure Analysis, 2009. **16**(1): p. 521-532.
13. Elforjani, M. and D. Mba, *Accelerated natural fault diagnosis in slow speed bearings with Acoustic Emission.* Engineering Fracture Mechanics, 2010. **77**(1): p. 112-127.